Journal of Marine Science and Technology

Volume 26 | Issue 1 Article 12

# TOWARDS AN INTEGRATED STORM SURGE AND WAVE FORECASTING SYSTEM FOR TAIWAN COAST

Yeayi Peter Sheng
*University of Florida, Gainesville, Florida, U.S.A*, pete.pp@gmail.com

Vladimir Alexander Paramygin
*University of Florida, Gainesville, Florida, U.S.A.*

Chuen-Teyr Terng
*Central Weather Bureau, Taipei, Taiwan, R.O.C.*

Chi-Hao Chu
*Central Weather Bureau, Taipei, Taiwan, R.O.C.*

# TOWARDS AN INTEGRATED STORM SURGE AND WAVE FORECASTING SYSTEM FOR TAIWAN COAST

## Acknowledgements

Central Weather Bureau provided the field data used for model verification in this paper. We appreciate the comments of two anonymous reviewers.

*Journal of Marine Science and Technology, Vol. 26, No. 1, pp. 117-127 (2018)*
DOI: 10.6119/JMST.2018.02_(1).0011


# TOWARDS AN INTEGRATED STORM SURGE AND WAVE FORECASTING SYSTEM FOR TAIWAN COAST

Yeayi Peter Sheng[1], Vladimir Alexander Paramygin[1],
Chuen-Teyr Terng[2], and Chi-Hao Chu[2]

Key words: storm surge, wave, numerical simulation, forecasting, Taiwan.

## ABSTRACT

This paper describes the application of a coupled surge-wave model for simulating storm surge and wave along Taiwan coast. The simulations were conducted with an integrated surge-wave modeling system using a large coastal model domain wrapped around the island of Taiwan, with a grid resolution of 50-400 m. Simulations were made with tide only, with wind and tide, and with tide and wind and wave.

The first part of the paper describes the hindcasting of historical typhoons. Hindcasting of Soudelor in 2015 revealed the significant effect of waves on storm surge when wave exceeded 11 m. Both the water level and wave were well simulated by the surge-wave model. The second part of the paper describes the forecasting of typhoons in 2016 With a focus on typhoon Napartak and Megi to examine the reliability, accuracy, and efficiency of the protopype forecasting system for Taiwan coast.

The system uptime is estimated at 78% during the three months of operations. While the tide prediction has about 3-10% error (relative root-mean-square-error), the water level prediction error increases from 5.8-13.5% for now cast to 9.8-17.4% for 6-hour forecast, 11.4-18.2% for 12-hour forecast, and 20.3-31.4% for 24-hour forecast. The forecast error increases quickly for 24-hour forecast, due to the quick decline of typhoon track/intensity forecast accuracy beyond 24 hours. The forecasting system is run using an Intel-based PC with the Intel® Core™ i7-3770 CPU @ 3.40 Ghz (4 cores/8 threads) with 32GB RAM. Wall time varies between 0.8 and 1.8 hours.

*Paper submitted 02/13/17; revised 07/24/17; accepted 09/07/17. Author for correspondence: Y. Peter Sheng (e-mail: pete.pp@gmail.com).*
*[1] University of Florida, Gainesville, Florida, U.S.A.*
*[2] Central Weather Bureau, Taipei, Taiwan, R.O.C.*

## I. INTRODUCTION

More than 75% of the world's population live within 100 miles from the coastline. Coastal communities and ecosystems around the world are subjected to increasing hazard from storm surge and coastal inundation due to tropical cyclones as well as climate change and sea level rise. In Taiwan typhoons are an annual threat. Not only bringing torrential rain, but often cause storm surge and coastal inundation that impacts areas near the coast and amplifies the flooding from rainfall. The impact of tropical cyclones on the coastal regions in Taiwan depend on the tropical cyclone characteristics and coastal region characteristics. For example, along the southwest coast of Taiwan with low elevation and gentler bathymetric slope, major flooding often occurs due to storm surge during tropical cyclones. Typhoon Fanapi caused major flooding along the southwest coast of Taiwan in September 2010. Along the rocky northeast coast of Taiwan where the bathymetric slope is steep, waves often break very close to the coastline and contribute significantly to the storm surge. During July 2013, Typhoon Soulik cuased significant storm surges and waves along the northeast coast of Taiwan. This is also true for Typhoon Soudelor (2015). Although storm surge is typically not as high as waves along the coast of Taiwan, rising sea level and increasingly more intense typhoons are mostly likely to result in higher storm surge in the 21st century which, coupled with increasing precipitation and subsidence in southwest Taiwan, could significantly increase the risk of coastal flooding in Taiwan. Therefore, a robust storm surge and wave forecasting system for Taiwan is urgently needed.

Numerous storm surge studies have been conducted around Taiwan using a number of different storm surge models, e.g., CWB-1 model (Yu et al., 1994), CWB-2 model (Wu, 2014), TORI (Taiwan Ocean Research Institute) model (Liau and Chen, 2015), and HMTC (Harbor and Marine Technology Center) model (Lee et al., 2015). According to a review by Sheng (2015), these models did not include wave effects. In addition, the grid resolution of the CWB-1 and CWB-2 are relatively coarse (> 200 m). These factors contributed to the relatively large errors in the storm surge simulation during past typhoons including

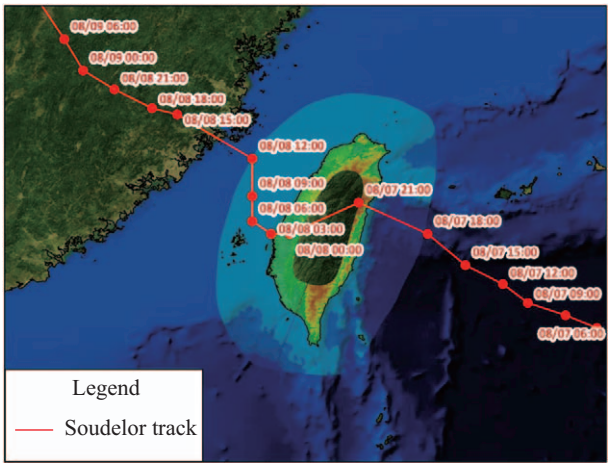


**Fig. 1. Computational domain and track of Typhoon Soudelor in 2015.**

Fanapi in 2010 and Soulik in 2013. Sheng et al. (2016) has shown that coupled wave-surge model can significantly improve the water level predictions where waves play a major role.

This paper uses an integrated storm surge modeling system (Sheng et al., 2010a, 2010b) to simulate storm surge and coastal inundation during typhoon Soudelor (2015). The simulations use a coastal model domain (Fig. 1) wrapped around the island of Taiwan with a grid resolution of 50-300 m coupled to a larger rectangular domain to provide boundary conditions for the simulation capturing surge and waves away from the coast. The same basic modeling system, with appropriate supporting modules, is used to forecast the storm surge and wave during 2016 and results during Nepartak and Megi are presented in this paper. The reliability, accuracy, and efficiency of the prototype forecasting system is assessed.

## II.TYPHOONS IN 2015 AND 2016

We describe Typhoon Soudelor in 2015 and Typhoon Nepartak and Megi in 2016 below.

### 1. Typhoon Soudelor (2015)

Typhoon Soudelor (Wikipedia, 2017) was the most intense tropical cyclone to develop in the Pacific Ocean and the third most intense cyclone worldwide in 2015, and the strongest typhoon since Typhoon Vongfong. Soudelor had severe impacts in the Northern Mariana Islands, Taiwan, and eastern China, resulting in at least 38 confirmed fatalities. Lesser effects were felt in Japan, South Korea and the Philippines. Soudelor formed as a tropical depression on July 29 near Pohnpei and was the thirteenth named storm of the 2015 typhoon season. It was slowly strengthening and several days later started intensifying on August 2.

The center of the storm made landfall in eastern Taiwan at 04:40 a.m. local time on August 8. By about 9 a.m., Soudelor had maximum sustained winds of 173 km/h, according to Taiwan's Central Weather Bureau (CWB-MMC). Winds caused Taipei 101's tuned mass damper to sway a record 100 cm. Yilan County in eastern Taiwan experienced the heaviest rains from the typhoon, with accumulations peaking at 1,334 mm. Rainfall in the Wulai District reached 722 mm in 24 hours. Twelve-hour accumulations amounted to a record 632 mm.

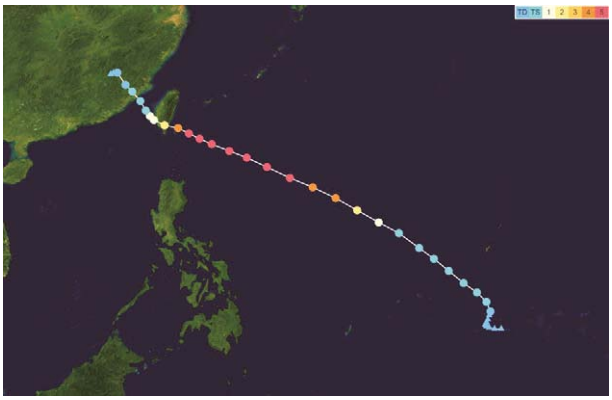

**Fig. 2. Typhoon Nepartak (2016) track.**

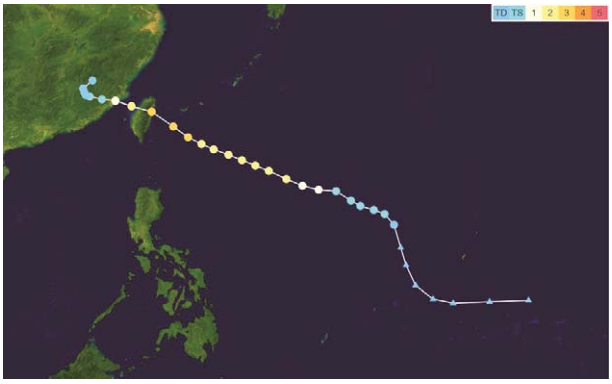

**Fig. 3. Typhoon Megi (2016) track.**

### 2. Typhoon Nepartak (2016)

Typhoon Nepartak (Fig. 2) is the second most intense tropical cyclone in 2016 in terms of atmospheric pressure. Nepartak severely impacted Taiwan and East China, with 86 confirmed fatalities. It caused 3 deaths and NT$677 million (US$21.1 million) of damage in Taiwan. The first named storm and typhoon of the annual typhoon season, Nepartak developed into a tropical storm south of Guam on July. Steadily tracking northwestward and becoming a typhoon on the next day, Nepartak reached peak intensity with a pinhole eye on July 6. Nepartak started to decay on July 7 and then crossed Taiwan later, before emerging into the Taiwan Strait and weakening into a severe tropical storm on July 8. It eventually made landfall over Fujian, China on July 9 and dissipated over land one day later.

### 3. Typhoon Megi (2016)

Typhoon Megi (Fig. 3), known in the Philippines as Typhoon Helen, was a large and powerful tropical cyclone which affected Taiwan and China in late September 2016. It is the seventeenth named storm and the seventh typhoon of the annual typhoon season.

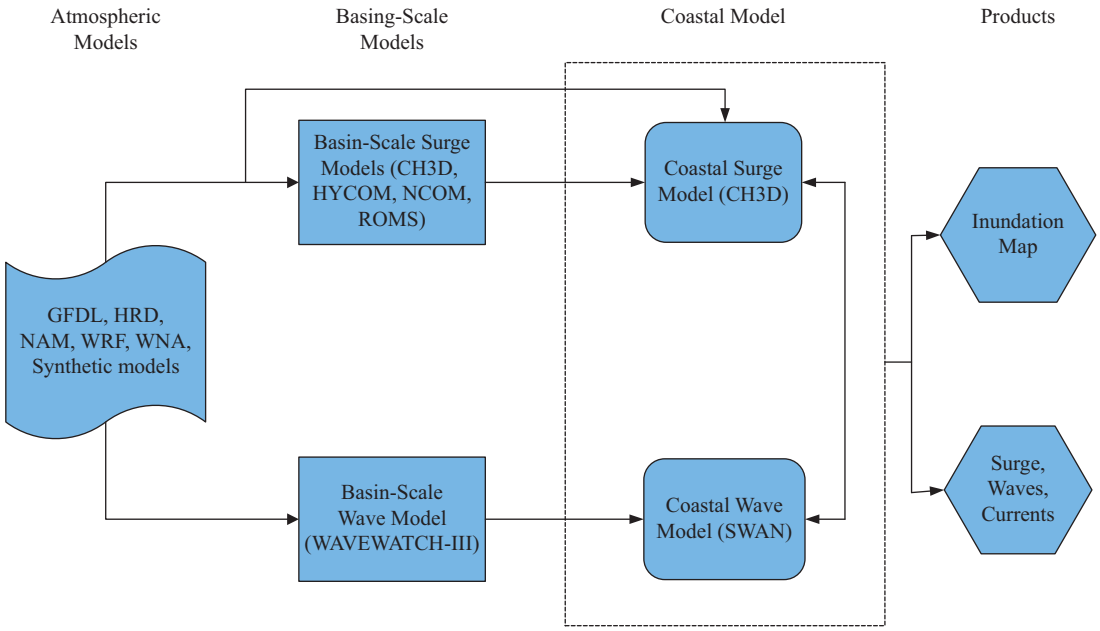


**Fig. 4. Basic schematic diagram of the ACMS.**

A tropical disturbance formed northeast of Pohnpei on September 19. Two days later, the Japan Meteorological Agency (JMA) upgraded the low-pressure area to a tropical depression early on September 21, and the Joint Typhoon Warning Center (JTWC) also issued a Tropical Cyclone Formation Alert shortly after that; however, the low-level circulation center (LLCC) of that disorganized system was exposed with fragmented convection. The JMA upgraded the system to a tropical storm and named it Megi early on September 23, when the JTWC also indicated that the monsoonal circulation had consolidated, resulting in upgrading it to a tropical depression but lacking of a definitive center. Six hours later, the JTWC upgraded Megi to a tropical storm.

On September 26, the JMA indicated that Megi had reached its peak intensity at 18:00 UTC, with ten-minute maximum sustained winds at 155 km/h (100 mph) and the central pressure at 940 hPa (27.76 inHg). Megi's large eye was temporarily more defined early on September 27; however, it soon became cloud-filled as the typhoon had approached the eastern coast of Taiwan. Shortly before Megi made landfall over Hualien City at 14:00 NST (06:00 UTC), it had already intensified into a stronger typhoon at around 03:00 UTC, with one-minute maximum sustained winds at 205 km/h (125 mph) indicated by the JTWC, equivalent to Category 3 of the Saffir-Simpson hurricane wind scale. Subsequently, interaction with the high mountains of Taiwan caused Megi to weaken significantly and the typhoon emerged into the Taiwan Strait from Mailiao at 21:10 NST (13:10 UTC). At 04:40 CST on September 28 (20:40 UTC on September 27), Megi made landfall over Hui'an County of Quanzhou, China as a minimal typhoon.

## III. NUMERICAL MODEL AND SETUP

### 1. ACMS Modeling System

This study uses the Advanced Coastal Modeling System (ACMS, see Fig. 4) which is an integrated storm surge modeling system (Sheng et al., 2006, 2008, 2010a, 2010b; Sheng and Liu, 2011; Tutak and Sheng, 2011) built upon the CH3D (Curvilinear-grid Hydrodynamics in 3D) circulation model (Sheng, 1987; Sheng, 1990). The CH3D model solves the continuity equation and the horizontal momentum equations in non-orthogonal boundary-fitted horizontal coordinates and a sigma coordinate system in the vertical dimension, making it suitable for complex coastal zone applications. CH3D can be run in both 3D and 2D vertically integrated modes. A robust turbulence closure model (Sheng and Villaret, 1989) is used to represent vertical mixing, while horizontal mixing is represented with Smagorinsky type mixing coefficients. A flooding and drying algorithm based on an enhanced version of Davis and Sheng (2003) is included in the model to enable accurate storm surge and inundation simulation. At the air-sea interface, the shear stress is produced by wind as well as waves, while at the bottom, current-wave interaction produces enhanced bottom stress. Detailed motion and boundary condition equations are described in Sheng et al. (2010a).

The ACMS has the capability of using a variety of wind fields and related boundary conditions as forcing, including the GFDL (Geophysical Fluid Dynamics Laboratory) model (Kurihara et al., 1998), NOAA (National Oceanic and Atmospheric Administration)/HRD (Hurricane Research Division) H* (e.g., DiNapoli et al., 2012), NAM (North Atlantic Mesoscale) model which is basically the WRF (Weather Research and Forecast) model operated by the National Center for Environmental Prediction (NCEP) at the U.S., NOGAPS (Navy Operational Global Atmospheric Prediction System, see Rosmond 1992), Advanced Research WRF model (http://www2.mmm.ucar.edu/wrf/users/docs/user_

guide_V3/contents.html), TWRF (Hsiao et al., 2010, 2012) etc. In addition, the ACMS implements several parametric synthetic wind models such as Wilson (1960), Holland (1980), and Xie, et al. (2006). It also has the capability to add wind dissipation due to land roughness based on land cover data (IPET 2008, Sheng et al., 2010b), and wind data assimilation.

In the ACMS, the CH3D model is dynamically coupled to the SWAN (Simulating WAves Nearshore) wave model (Ris et al., 1999): wave results obtained by SWAN are passed to the CH3D and water depths and currents obtained by the CH3D model are passed onto SWAN. This allows accounting for wave setup and wave-current interaction within the CH3D model, which features several formulations for calculating wave stresses, including vertically varying formulations (e.g., Mellor 2008) as well as the vertically uniform formulation of Longuet Higgins and Stewart (1962, 1964). For simplicity, however, vertically uniform wave stress formulation is used in this study. Operationally, the CH3D model is run every 15-30 minutes and its results passed to SWAN for wave simulation once and its results passed back to CH3D. This process repeats itself throughout the forecast cycle.

The ACMS uses a high resolution horizontal grid that can vary from 20-30 m near the coast to a few hundred meters in offshore areas. Because it uses an efficient implicit/semi-implicit algorithm to resolve surface gravity wave propagation, CH3D allows the use of relatively large time steps (1-60 s). To maintain high efficiency in CH3D simulations, a high resolution grid is usually used only in the coastal domain, which extends from the coastline to 50-100 km offshore. The coastal domain is usually coupled to a basin scale (large scale) domain which covers all or part of a large basin, e.g., the Gulf of Mexico, or the Northwest Pacific Ocean, which can be simulated using a variety of ocean circulation models, e.g., CH3D, NCOM (Barron et al., 2004), HYCOM (Bleck and Benjamin, 1993) etc. While NCOM (Navy Coastal Ocean Model) and HYCOM (HYbrid Coordinate Ocean Model) do not simulate tides, CH3D can be used to simulate both tides and storm surge during typhoons in the coastal domain.

ACMS, which is also known as CH3D-SSMS (CH3D-Storm Surge Modeling System), has been compared to other storm surge models including ADCIRC (ADvanced CIRCulation Model; Luettich et al., 1992), CMEPS (Peng et al., 2004), FVCOM (Finite Volume Coastal Ocean Model; Chen et al., 2006), and SLOSH (Sea, Lake and Overland Surges from Hurricanes; Jelesnianski et al., 1992). Detailed comparison of models (Sheng et al., 2012) were made in terms of simulated storm surges during historic storms as well as coastal inundation maps including the surge atlas and the 1% annual chance coastal inundation maps which is also known as the Base Flood Elevation (BFE) according to the Federal Emergency Management Agency (FEMA) of the US (NAS 2009).

## 2. Model Domains

For ACMS simulations, this study uses two computational domains which differ in area covered and horizontal resolution.

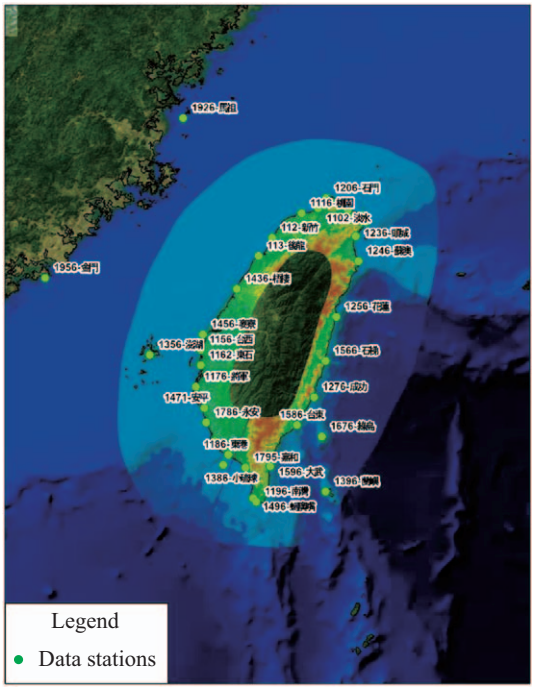


**Fig. 5. ACMS-TW Model Domain.**

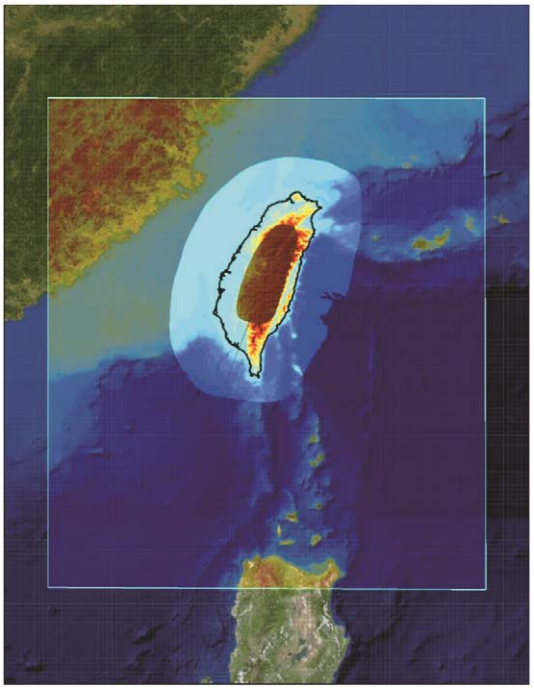

**Fig. 6. ACMS-TW500 Domain including the ACMS-TW domain.**

The smaller domain ACMS-TW, as shown in Fig. 5, covers the entire Taiwan Island coastline, containing 2 million grid cells with an average grid cell size of 150 m but a minimum grid of 50 m. This computational domain is nested inside a large rectangular domain ACMS-TW500, as shown in Fig. 6, with 500 m by 500 m grid resolution, which provides boundary conditions

to the TW domain. The ACMS-TW500 domain is always run in 2D mode and is only forced by wind and pressure fields and does not include the tide effects. Its purpose is to capture the larger scale effects of a typhoon. The SWAN model is run within the ACMS-TW domain and is dynamically coupled to the CH3D model. Both CH3D and SWAN use the same curvilinear grid with flooding and drying.

Bathymetry and topography for the model domain are derived from a dataset with 200 m horizontal resolution. CH3D model uses sigma vertical coordinates and 3D simulations discussed in this paper are carried out using eight vertical sigma layers.

The data stations located over the Taiwan coastline are shown in Fig. 5. For simplicity, selected model results at only a number of select stations where storm surge effects are most prominent are shown and discussed.

## 3. Initial Conditions

Numerical simulations are started with water level located at the mean sea level and a 2-day spin-up time allows tides to fully develop and properly initialize the water level before the storm reaches the model domain.

## 4. Tide Forcing

The water level at the open boundary of the TW domain consists of two components—surge and tides. The surge along the open boundary are simulated water level from the TW500 domain. TW500 model simulations are always done in 2D and are only forced by wind and sea level air pressure (tides are not included).

Along the open boundary of TW tidal constituents are extracted from the TPXO model (http://volkov.oce.orst.edu/tides/tpxo8_atlas.html) and the following constituents are used:

Primary: M2, S2, N2, K2, K1, O1, P1, Q1
Long period: Mf, Mm
Non-linear: M4, MS4, MN4

These constituents are locally adjusted to provide a better fit to local data. Tides are verified by running a no-wind scenario and comparing simulated tides against the prediction values (only five major constituents: K1, M2, N2, O1, S2 areprovided by CWB for verification) against measured data and verification results are displayed in Fig. 7. The surge and tidal boundary conditions are then combined to form an open boundary condition for the ACMS-TW domain. The tidal verification, which was conducted during the study of Typhoon Fanapi, is provided here as an example to show the generally good tidal prediction by the ACMS-TW system.

Wave boundary conditions at the open boundary are drawn from SWAN results on the ACMS-TW500 domain.

To examine the impact of large scale circulation on coastal currents during typhoons, it is possible for our model to use the results from the large scale ocean circulation model (e.g., Ko et al., 2016) as open boundary conditions.

## 5. Wind Forcing

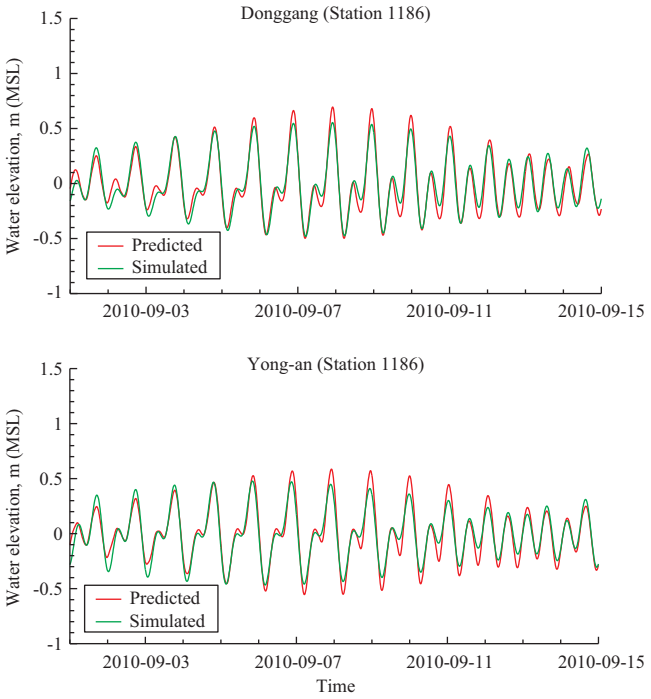


**Fig. 7. Simulated vs. measured tides at two stations.**

Three different wind models could be used to force the coastal modeling system:

1. An analytical parametric wind model with some modifications from Xie et al. (2006). This model is driven by such storm parameters as: location of the center of the storm, central pressure, maximum wind speed and several radii to constant wind. Four radii are defined for each constant wind contour (one for each quadrant) giving the wind field an assymetric shape. The wind field is then calculated as a function that is fit to these parameters. All parameters are obtained from best tracks provided by the CWB and the US Navy Joint Typhoon Warning Center
2. An analytical parametric wind model originaly designed by Holland (1980). This model is also driven by parameters from the best track, but the wind field is defined using the following parameters: location of the storm center, pressure in the center of the storm, translational speed of the storm, maximum wind speed and the radius to maximum wind. All parameters are obtained from best tracks provided by the CWB and the US Navy Joint Typhoon Warning Center.
3. The Weather Research and Forecasting (WRF) model (e.g., Skamarock et al., 2005, Hsiao et al., 2010) which is a next-generation mesoscale numerical weather prediciton system. Wind snapshots output from the TWRF model at 6-hour intervals provided by the Central Weather Bureau (Hsiao et al., 2010) were used to define the wind forcing.

For parametric wind models, wind dissipation by land cover and land use features is usually applied to the wind profiles,

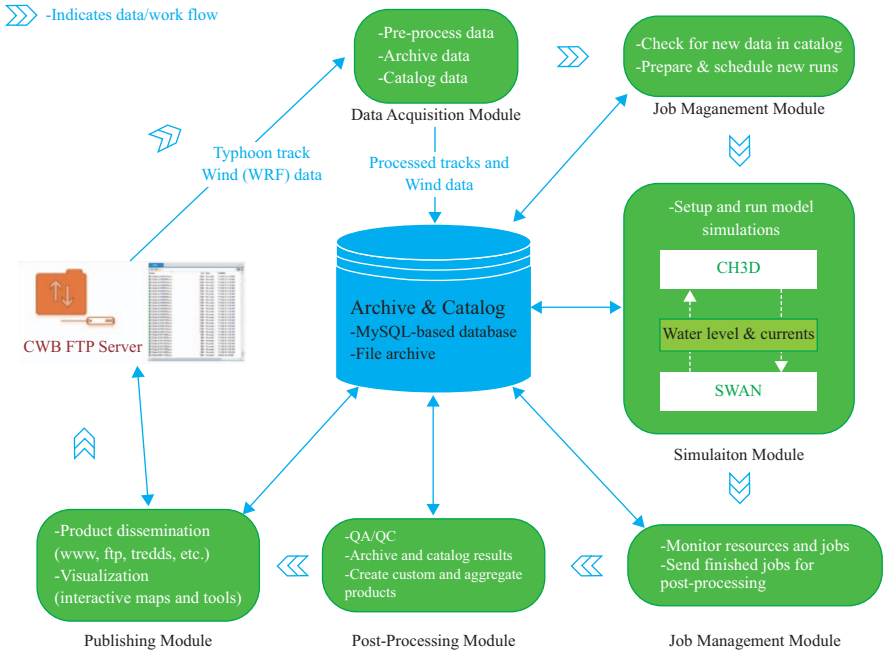


**Fig. 8. Workflow/Dataflow diagram of ACMS-TW Forecastign System in 2016.**

following the procedure described in Interagency Performance Evaluation Task Force (IPET, 2008) and Sheng et al. (2010b). However, due to lack of high resolution land data for this study, the detailed land dissipation procedure is not used. Instead, a simpe wind reduction factor, based on the logrithmic wind profile above the land surface vs. water surface, is applied to the typhhon wind over water to calculate the over-the-land wind.

When parametric wind models are used, wind fields are updated at every model timestep. For the WRF-driven model runs, wind fields are interpolated using a method that takes into account the position of the storm from 6-hourly wind fields (see, e.g., Sheng et al., 2010a).

Available wind observations are limited, especially given the fact that models use wind at 10 m elevation but available observed data is at 1-5m elevation, an adjustment is needed in order to compare the simulated to observed wind. Moreover, the TWRF wind fields were provided to us very late in the typhoon season, hence no comparison of the three wind fields were made in this study. The forecasting results presented below are based on the CWB typhoon tracks and the Holland (1980) wind field.

## 6. Model Parameters

CH3D model runs in 2D and 3D modes are made. The 2-D model uses Manning's bottom friction formulation with the Manning's n = 0.025. The 3-D model uses 4 vertical sigma layers and a bottom roughness $Z_0$ = 0.4 cm. As explained in Lapetina and Sheng (2015), these values are typical values for storm surge model simulations. Both two-dimensional and three-dimensional models use a 30-second time step.

## 7. Prototype ACMS-TW Forecasting System

The basic ACMS as described above has been applied to simulate historical typhoons in Taiwan, including Fanapi (2010) and Soulik (2013), as shown in Sheng et al. (2016). In July-September 2016, the ACMS-TW modeling system was used in a forecasting mode to test the feasibility of using ACMS-TW for longterm forecasting of storm surge and wave along the Taiwan coast.

As shown in Fig. 8, the system consists of several modules:

(1) Data Acquisition Module: This module collects, analyzes data and performs pre-processing. The module monitors the CWB-MMC FTP site (where typhoon track information is stored by CWB) by connecting with it every 5 minutes and checking for new file contents. New files are downloaded and compared to existing data (since track files can be duplicated). If new data is found, the files are converted to internal format, saved in the archive and records are added to the catalog database. A new simulation is then prepared by creating appropriate input files for CH3D and SWAN models.

(2) Job Management Module: This module monitors the database for newly created simulations, polls existing simulations and marks them up for post-processing when finished. It utilizes HTCondor to submit/poll/cancel and re-submit jobs. Optional support for prioritizing certain simulation scenarios and/or computing resources is available.

(3) Simulation Module: Consists of CH3D and SWAN model executables and their service utilities that are used to perform model runs.

(4) Post-Processing Module: This module post-processes the data for finished runs. A variety of output options are available such as ASCII output files (tab delimited, comma-separated, etc.), NetCDF (with CF conventions), ESRI Shape-

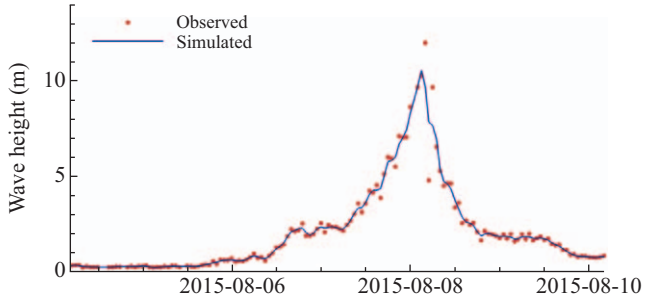


**Fig. 9. Observed vs predicted wave height at station 46699a (Hualien) during typhoon Soudelor.**

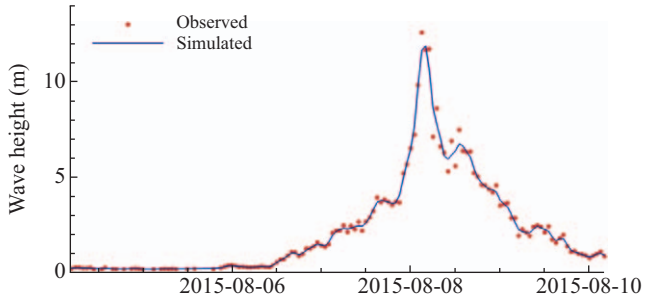


**Fig. 10. Observed vs predicted wave height at station 46708a (Guishandao) during typhoon Soudelor.**

files, Google KML files, etc. Converted files are stored in the archive and cataloged.

(5) Publishing Module: Consists of software which handles data publishing and dissemination. Many options are available via a THREDDS server serving NetCDF files which can be manipulated on the fly. ACMS-TW can publish results on the web in the form of maps, time-series plots and downloadable products in a variety of user-friendly formats. Current implementation of ACMS-TW uploads r.L and ss.L files to the CWB-MMC FTP site along with 12-hour averaged maximum tide, water level, and difference snapshot files.

Operation of the ACMS-TW forecasting system in 2016 consists of the following steps:

1. CWB-MMC places forecast tracks and TWRF winds on their FTP server.
2. ACMS-TW monitors the CWB-MM FTP server and downloads new data when available. New data triggers new simulations.
3. Each new dataset triggers a start of two new simulations (scenarios):
   (a) simulation forced only by astronomical tides
   (b) simulation forced by astronomical tides + wind and atmospheric pressure
4. ACMS runs a nowcast for to fill the gap between the previous dataset that was available and the current one, usually 6 hours, but it can vary. Both tide-only and full scenarios are done.

**Table 1. Water level RRMSE (Relative Root-Mean Square Error) (%) based on nowcast ACMS-TW simulations of Nepartak.**

| Station Name | Station ID | Station Name | Tide only | Hindcast |
|---|---|---|---|---|
| 龍洞 | 1226 | LONGDONG | 5.1 | 10.1 |
| 基隆 | 1516 | KEELUNG | 7.7 | 10.6 |
| 福隆 | 1821 | FULONG | 4.5 | 10.2 |
| 頭城 | 1236 | TOUCHENG | 5.0 | 10.4 |
| 蘇澳 | 1246 | SUAO | 4.0 | 12.0 |
| 花蓮 | 1256 | HUALIEN | 5.1 | 12.7 |
| 石梯 | 1566 | SHITI | 3.5 | 11.2 |
| 成功 | 1276 | CHENGKUNG | 4.1 | 11.1 |
| 台東 | 1586 | TAITUNG | 6.8 | 11.8 |
| 大武 | 1596 | DAWU | 8.2 | 12.2 |
| 綠島 | 1676 | LUDAO | 11.3 | 13.5 |
| 石門 | 1206 | SHIHMEN | 4.8 | 10.3 |
| 淡水 | 1102 | DANSHUEI | 4.4 | 10.3 |
| 桃園 | 1116 | TAOYUAN | 3.9 | 10.8 |
| 新竹 | 112 | HSINCHU | 3.2 | 11.3 |
| 後龍 | 113 | HOULONG | 5.0 | 11.0 |
| 芳苑 | 1456 | FANGYUAN | 4.1 | 10.5 |
| 台西 | 1156 | TAISI | 3.0 | 9.0 |
| 安平 | 1786 | ANPING | 4.0 | 9.8 |
| 嘉和 | 1386 | JIAHE | 4.0 | 8.6 |
| 蟳廣嘴 | 1496 | SUNGUANGZUEI | 3.5 | 7.7 |
| 南灣 | 1196 | NANWAN | 3.8 | 7.8 |
| 澎湖 | 1356 | PENGHU | 3.3 | 5.8 |

5. ACMS forecast for 48 hours starting from the last timestep of the nowcast. Both tide-only and full scenarios are done.
6. ACMS plots 12-hour maximum values (as contours) of maximum water level, maximum tide (tide-only simulation) and difference between the two.
7. ACMS outputs r.L and ss.L files containing time-series of tide and surge at 32 stations.
8. ACMS plots time-series plots of water levels of the two scenarios: tide-only and full at 32 stations.
9. ACMS uploads the plots and output files from steps 5-8 to the:
   (a) CWB-MMC FTP server and
   (b) ACMS server

## IV. MODEL RESULTS

### 1. Hindcasting of Soudelor (2015)

Soudelor produced very large waves along the northeastern coast of Taiwan. Observed and simulated wave heights exceeded 11m at Hualien and Guishangdao coast, as shown in Figs. 9 and 10, respectively. Observed water level at all stations are shown to be well simulated by the ACMS-TW modeling system (Fig. 11) with relative root mean square errors between 3-13%. Unfortunately there were missing data at key stations to allow detailed verification of wave effects on storm surge.

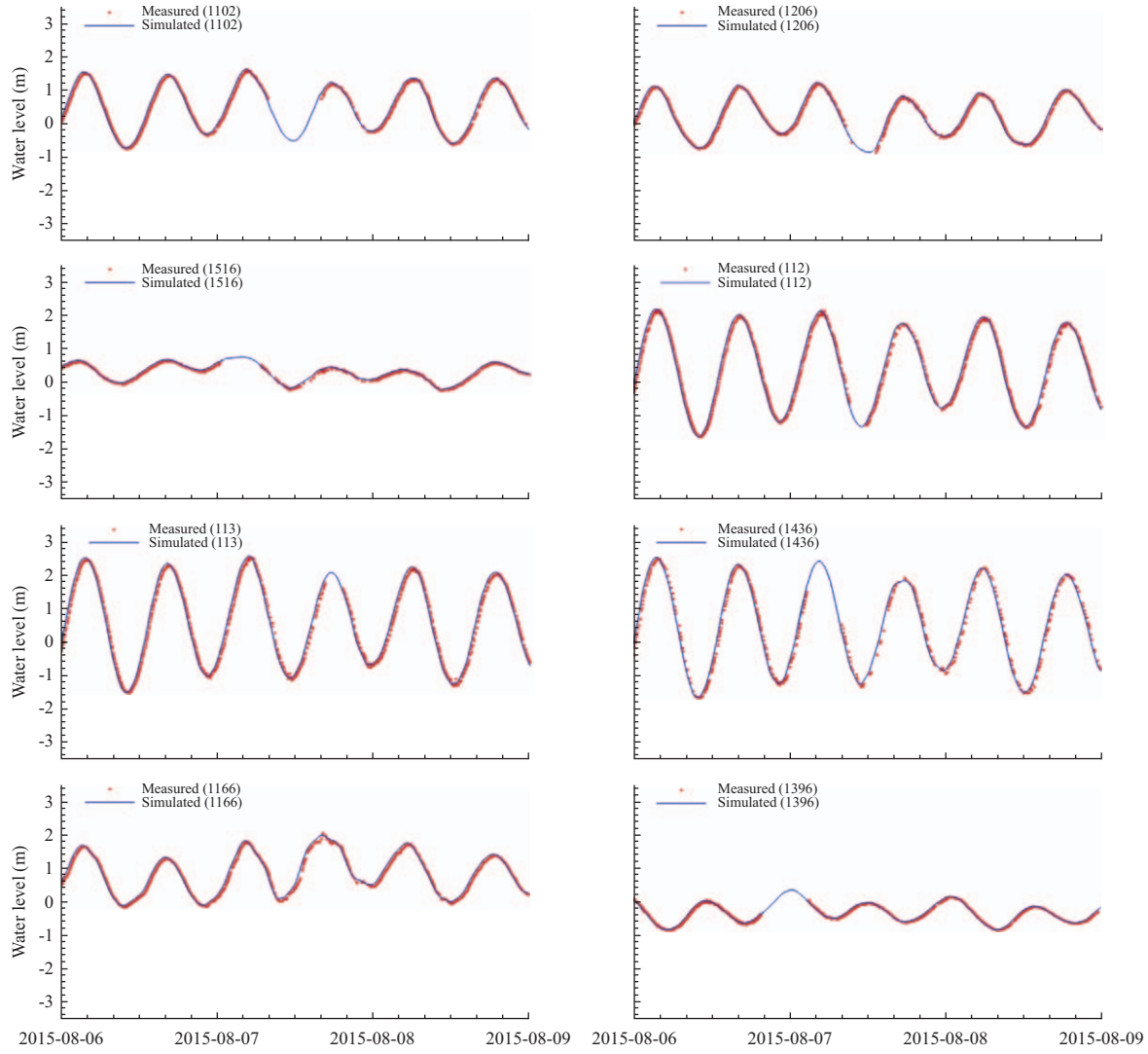


**Fig. 11. Simulated vs. measured water level at various stations during typhoon Soudelor. Simulated results are based on CH3D model simulations coupled with waves effects from the SWAN model.**

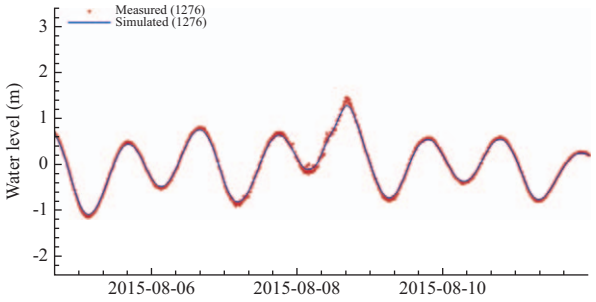


**Fig. 12. Simulated vs. measured water level at station 1276 (成功) during Napartak.**

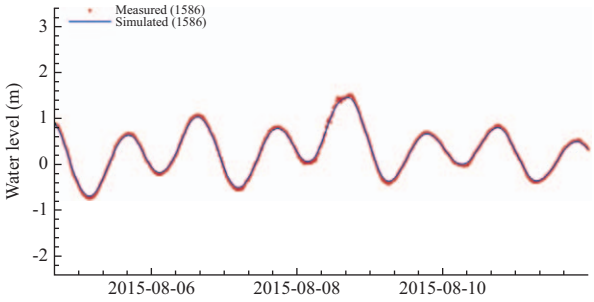


**Fig. 13. Simulated vs. measured water level at station 1586 (台東) during Nepartak.**

## 2. Forecasting of Nepartak and Megi (2016)

Simulated and observed water level during Nepartak are shown for Station 2176 and 1686 in Figs. 12 and 13, respectively. Simulated and observed wave height at two stations are shown in Figs. 14 and 15.

Relative Root Mean Square Errors (RRMSEs), which is the RMSE divided by the local maximum value, of simulated water level are compared for all the stations in Table 1 and Table 2.

**Table 2. Water level RRMSE (Relative Root-Mean-Square-Error) (%) based on 6-hour, 12-hour and 24-hour ACMS-TW forecasts of Nepartak.**

| Station Name | Station ID | Station Name | 6-hour forecast | 12-hour forecast | 24-hour forecast |
|---|---|---|---|---|---|
| 龍洞 | 1226 | LONGDONG | 13.1 | 14.0 | 30.0 |
| 基隆 | 1516 | KEELUNG | 13.8 | 13.9 | 27.6 |
| 福隆 | 1821 | FULONG | 13.0 | 14.4 | 30.1 |
| 頭城 | 1236 | TOUCHENG | 15.1 | 17.8 | 28.6 |
| 蘇澳 | 1246 | SUAO | 14.8 | 16.7 | 23.8 |
| 花蓮 | 1256 | HUALIEN | 14.8 | 16.5 | 31.4 |
| 石梯 | 1566 | SHITI | 13.5 | 15.7 | 30.1 |
| 成功 | 1276 | CHENGKUNG | 14.7 | 16.2 | 27.2 |
| 台東 | 1586 | TAITUNG | 15.3 | 16.6 | 27.6 |
| 大武 | 1596 | DAWU | 15.3 | 17.3 | 28.4 |
| 綠島 | 1676 | LUDAO | 16.4 | 18.2 | 29.5 |
| 石門 | 1206 | SHIHMEN | 13.9 | 15.0 | 26.6 |
| 淡水 | 1102 | DANSHUEI | 15.9 | 16.4 | 30.8 |
| 桃園 | 1116 | TAOYUAN | 13.9 | 17.4 | 31.0 |
| 新竹 | 112 | HSINCHU | 13.9 | 14.3 | 27.8 |
| 後龍 | 113 | HOULONG | 16.6 | 15.6 | 28.8 |
| 芳苑 | 1456 | FANGYUAN | 13.7 | 14.7 | 26.0 |
| 台西 | 1156 | TAISI | 9.8 | 16.5 | 27.6 |
| 安平 | 1786 | ANPING | 14.6 | 11.4 | 22.0 |
| 嘉和 | 1386 | JIAHE | 10.5 | 13.3 | 21.9 |
| 蟳廣嘴 | 1496 | SUNGUANGZUEI | 13.0 | 13.7 | 23.1 |
| 南灣 | 1196 | NANWAN | 13.0 | 16.0 | 20.5 |
| 澎湖 | 1356 | PENGHU | 17.4 | 18.1 | 25.1 |

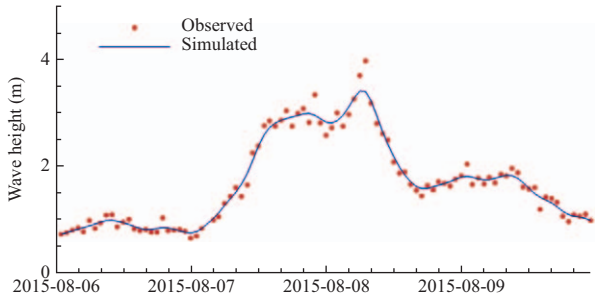


**Fig. 14. Simulated vs. measured wave height at station 46699a (花蓮) during Nepartak.**

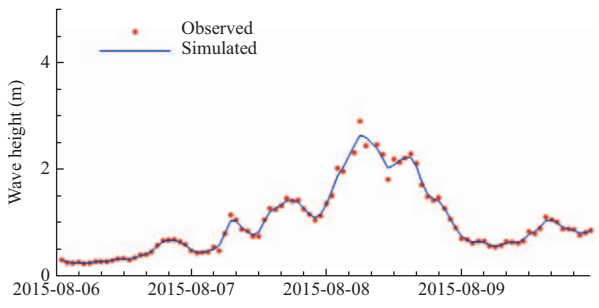


**Fig. 15. Simulated vs. measured wave height at station 46708a（龜山島） during Nepartak.**

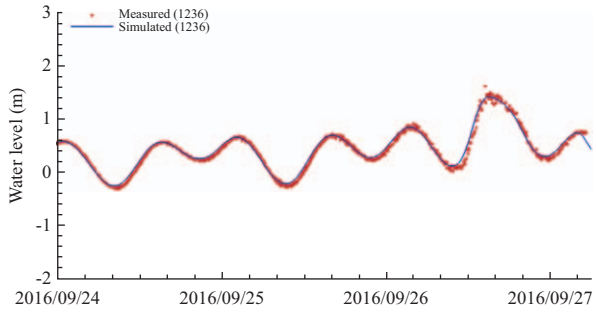


**Fig. 16. Simulated vs. measured water level at station 1236 (頭城) during Megi.**

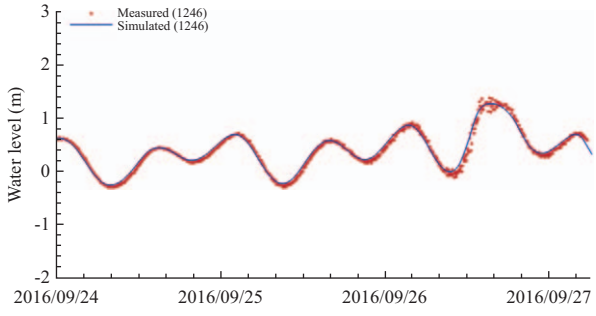


**Fig. 17. Simulated vs. measured water level at station 1246 (蘇澳) during Megi.**

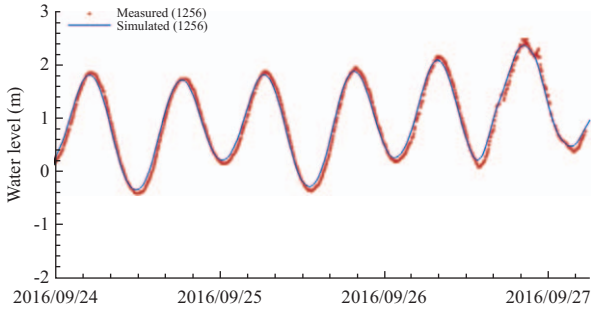


**Fig. 18. Simulated vs. measured water level at station 1156 (台西) during Megi.**

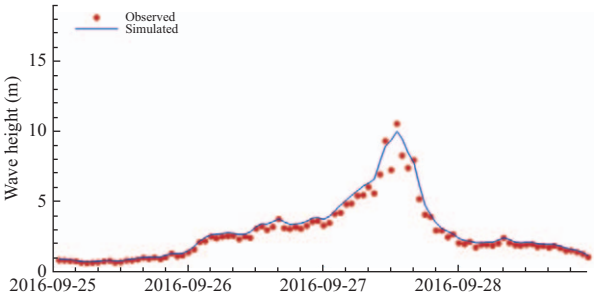


**Fig. 19. Simulated and observed wave height at Station 46609 (花蓮) during Megi.**

As shown in Table 1, the relative RMS error of simulated results are 3-8% for tidal simulation, 5.8-13.5% for water level hindcasting, while Table 2 shows 9.8-17.4% RRMSE for 6-hour forecast, 11.4-18.2% for 12-hour forecast, and 20.5-31.4% for 24-hour forecast. The sharp increase in RRMSE for 24-hour forecast is due to the sharp increase in the forecast track error.

Forecasting of Megi produced similar error statistics. 2.8-11.3% RRMSE for tide forecasting, 7.6-13.4% RRMSE for hindcasting/nowcasting, 9.9-16.6% for 6-hour forecast, 13.8-18% for 12-hour forecast, and 20.3-30.8% for 24-hour forecast. Simulated and observed water level at three stations are shown below in Figs. 16-18. Simulated and observed wave height at Hualien reached 10 m (Fig. 19), while wave height at Suao was almost 20 m (Fig. 20).

## V. FORECASTING EFFICIENCY AND PERFORMANCE

The forecasting system is run using an Intel-based PC with the Intel® Core™ i7-3770 CPU @ 3.40 Ghz (4 cores/8 threads) with 32GB RAM. Wall time varies between 0.8 and 1.8 hours.

Despite several issues with connectivity which caused the inability of system to acquire data and perform simulations, the system uptime is estimated at 78% during the three months of operations. A total of 578 CSV-formatted storm track files were issued between July 1 and September 30, 2016. 485 of these were unique, others were duplicate. 378 of these tracks were processed within 6 hours or less (within one cycle time of ACMS).

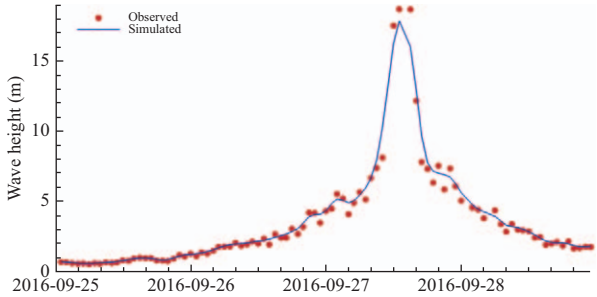


**Fig. 20. Simulated and observed wave height at Station 46706 (蘇澳) during Megi.**

107 tracks were processed late due to several issues which led to our inability to obtain tracks.

Connectivity issues will be resolved in future forecasting using ACMS-TW.

## VI. SUMMARY

ACMS-TW modeling system has been used for hindcasting of historical storms in 2015 and forecasting in July-September 2016. Simulation and observation of Typhoon Soudelor (2015) showed very high waves exceeding 11 m occurred along the northeast Taiwan coast. Simulated water level and wave agree quite well with observed data.

The accuracy of the ACMS-TW forecasting system is found to be quite satisfactory based on comparison between simulated and observed tide, water level, and wave. While the tide prediction has about 5% error (RRMSE), the 6-hour and 12-hour forecasts show 10-20% error. The forecast error increases to more than 20% for 24-hour forecasts. This is due to the fact that the typhoon track/intensity forecast accuracy declines quickly beyond 24 hours. Effort is needed to improve the typhoon track/intensity error. Alternatively, ensemble forecasting (e.g., Davis et al., 2012) using past forecast errors in intensity and track could improve the forecasting by showing the probabilistic forecasting results.

The ACMS-TW forecasting system could be expanded by adding a web-based interface to allow real-time tracking of system status following the system workflow. Additional output options with a THREDDS-based server could be added as well.

## ACKNOWLEDGEMENTS

Central Weather Bureau provided the field data used for model verification in this paper. We appreciate the comments of two anonymous reviewers.

## REFERENCES

Barron, C. N., A. B. Kara, H. E. Hurlburt, C. Rowley and L. F. Smedstad (2004). Sea surface height predictions from the Global Navy Coastal Ocean Model (NCOM) during 1998-2001. J. Atmos. Oceanic Technol 21, 1876-1894.

Bleck, R. and S. Benjamin (1993). Regional weather prediction with a model combining terrain-following and isentropic coordinates. Part I: Model de-

scription. Mon. Wea. Rev. 121, 1770-1785.

Chen, C., G. Cowles and R .C. Beardsley (2006). An unstructured grid, finite volume coastal ocean model: FVCOM User Manual, 2nd Ed. SMAST/ UMASSD Report TR-06-0602, 315.

Davis, J. R. and Y. P. Sheng (2003). A parallel storm surge model. International Journal of Numerical Methods in Fluids (Elsevier) 42, 549-80.

DiNapoli, S. M., M. A. Bourassa and M. D. Powell (2012). Uncertainty and intercalibration analysis of H*Wind. J. Atmos. Oceanic Technol. 29, 822-833.

Hsiao, L. F., C. S. Liou, T. C. Yeh, Y. R. Guo, D. S. Chen, K. N. Huang, C. T. Terng and J. H. Chen (2010). A vortex relocation scheme for tropical cyclone initialization in advanced research WRF. Mon. Wea. Rev., 138, 3298-3315.

Holland, G. J. (1980). An analytic model of the wind and pressure profiles in hurricanes. Monthly Weather Review 108, 1212-1218.

IPET (2008). Performance evaluation of the New Orleans and Southeast Louisiana hurricane protection system, Draft Final Report of the Interagency Performance Evaluation Task Force, US Army Corps of Engineers, USA.

Jelesnianski, C. P., J. Chen and W. A. Shaffer (1992). SLOSH: Sea, lake, and overland surges from hurricanes. NOAA Tech. Rep. NWS 48, 71.

Joint Typhoon Warning Center (2016). Tropical Cyclone Formation Alert. Joint Typhoon Warning Center. September 21, 2016. Archived from the original on September 21, 2016. Retrieved September 27, 2016.

Kang, N. and J. B. Elsner (2015). Trade-off between intensity and frequency of global tropical cyclones. Nature Climate Change 5, 661-664.

Kurihara, Y., R. E. Tuleya and M. A. Bender (1998). The GFDL hurricane prediction system and its performance in the 1995 hurricane season. Monthly Weather Review 126, 1306-1322.

Ko, D.-S., S.-Y. Chao, C.-C. Wu, I-I Lin and S. Jan (2016). Impacts of tides and typhoon Fanapi (2010) on Seas around Taiwan. Terrestrial, Atmospheric, and Oceanic Sciences 27(2), 261-280.

Lapetina, A. and Y. P. Sheng (2015). Simulating complex storm surge dynamics: Three-dimensionality, vegetation effect, and onshore sediment transport. J. Geophys. Res. - Oceans 120(11), 7363-7380.

Lee, J., Y. Chiu, C. Liu, C. Su, M. Cheng, J. Lee, L. Tu and C. Shieh (2015). Enhancement of marine meteorology simulation techniques for system maintenance and operation in Taiwan major harbors, Harbor & Marine Technology Center, Institute of Transportation, Ministry of Transportation and Communications. 104-005-7788, MOTC-IOT-103-H3DC001.

Liau, J.-M. and S.-H. Chen (2015). Effect of the wave set-up on the estimation of storm surge in the coastal waters. Taiwan Water Conservancy 63(1).

Longuet-Higgins, M. S. and R. W. Stewart (1962). Radiation stress and mass transport in gravity waves with application to 'surf beats'. Journal of Fluid Mechanics 13, 481–504.

Longuet-Higgins, M. S. and R. W. Stewart (1964). Radiation stresses in water waves; a physical discussion with applications. Deep-Sea Research 11, 529-562.

Luettich, R., J. J. Westerink and N. W. Scheffner (1992). ADCIRC: an advanced three-dimensional circulation model for shelves coasts and estuaries, report 1: theory and methodology of ADCIRC-2DDI and ADCIRC-3DL. DRP-92-6, U.S. Army Engineers Waterways Experiment Station, Vicksburg, MS, 137.

Mellor, G. L. (2008). The depth dependent current and wave interaction equations; a revision. J. Phys. Oceangr. 38, 2587-2596.

Ministry of Economy (2010). Investigative report of coastal flooding during typhoon Fanapi. Taiwan, ROC.

National Academy of Sciences (2009). Mapping the Zone - Improving Flood Map Accuracy, Committee on FEMA Flood Maps, National Research Council. 136.

Peng, M., L. Xie and L. J. Pietrafesa (2004). A numerical study of storm surge and inundation in the Croatan-Albemarle-Pamlico Estuary System. Estuarine Coastal Shelf Sci. 59, 121-137.

Ris, R. C., N. Booij and L. H. Holthuijsen (1999). A third-generation wave model for coastal regions, Part II, Verification. Journal of Geophysical Research 104, 7667-7681.

Rosmond, T. (1992). The Design and Testing of NOGAPS. Weather and Forecasting 7(2), 262-272.

Sheng, Y. P. (1987). On modeling three-dimensional estuarine and marine hydrodynamics. Three-dimensional models of marine and estuarine dynamics, Elsevier Oceanography Series (Editor: J. C. J. Nihoul and B. Jamart), Elsevier, 35-54.

Sheng, Y. P. (1990). Evolution of a three-dimensional curvilinear-grid hydrodynamic model for estuaries lakes and coastal waters: CH3D. Estuarine and Coastal Modeling I, ASCE, 40-49.

Sheng, Y. P. (2015). Evaluation of an integrated Taiwan coastal hazard forecasting system, Interim Report for Central Weather Bureau.

Sheng, Y. P. and C. Villaret (1989). Modeling the effect of suspended sediment stratification on bottom exchange process. Journal of Geophysical Research 94, 14229-14444.

Sheng, Y. P., V. A. Paramygin, V. Alymov and J. R. Davis (2006). A Real-time forecasting system for hurricane induced storm surge and coastal flooding. Estuarine and Coastal Modeling, Proc. Of the Ninth International Conference, ASCE, 585-602.

Sheng, Y. P., V. A. Paramygin, Y. Zhang and J. R. Davis (2008). Recent enhancements and application of an integrated storm surge modeling system: ACMS. Estuarine and coastal modeling. Proc. of the Tenth International Conference, ASCE, 879-892.

Sheng, Y. P., V. Alymov and V. A. Paramygin (2010a). Simulation of storm surge, waves, currents, and inundation during hurricane isabel in 2003. J. Geophys. Res. 115, 1-27.

Sheng, Y. P., Y. Zhang and V. A. Paramygin (2010b). Simulation of storm surge, wave, and coastal inundation in the Northeastern Gulf of Mexico region during Hurricane Ivan in 2004. Ocean Modelling 35, 314-331.

Sheng, Y. P. and T. Liu (2011). Three-dimensional simulation of wave-induced circulation: Comparison of three radiation stress formulations. J. Geophys. Res. 116, C05021.

Sheng, Y. P., J. R. Davis, R. Figueiredo, B. Liu, H. Liu, R. Luettich, V. A. Paramygin, R. Weaver, R. Weisberg, L. Xie and L. Zheng (2012). A regional testbed for storm surge and coastal inundation models - An Overview. Proceedings of the 12th International Conference on Estuarine and Coastal Modeling, American Society of Civil Engineers.

Sheng, Y. P., V. A. Paramygin, C. Chu and C. T. Terng (2016). Simulation of storm surge and wave during Typhoon Fanapi and Soulik along Taiwan coast. Terrestrial, Atmospheric, and Oceanic Sciences 22(6), 965-979.

Skamarock, W. C., J. B. Klemp, J. Dudhia, D. O. Gill, D. M. Barker, W. Wang and J. G. Powers (2005). A Description of the Advanced Research WRF Version 2.

Tutak, B. and Y. P. Sheng (2011). Effect of tropical cyclones on residual circulation and momentum balance in a subtropical estuary and inlet: Observation and simulation. J. Geophys. Res. 116, C06014.

Wikipedia (2017. https://en.wikipedia.org/wiki/Typhoon_Soudelor.

Wilson, B. W. (1960). Note on surface wind stress over water at low and high wind speeds. Journal of Geophysical Research 65, 3377-3382.

Wu, C. (2014). Development of a forecasting model for near coast storm surge and coastal inundation in Taiwan. Progress report fo Central Weather Bureau. MOTC-CWB-103-O-02.

Yu, C. S., M. Marcus and J. Monbaliu (1994). Numerical modeling of storm surges along the Belgium coast. In: Computational Methods in Water Resouces X, Peters et al. (eds), Water Science Technology Library, Kluwer Academic Publishers, Dordrecht, 1331-1338.

Xie, L., S. Bao, L. J. Pietrafesa, K. Foley and M. Fuentes (2006). A real-time hurricane surface wind forecasting model: Formulation and verification. Monthly Weather Review 134, 1355-1370.